

Electron Binding Motifs of $(\text{H}_2\text{O})_n^-$ Clusters

Thomas Sommerfeld and Kenneth D. Jordan*

Contribution from the University of Pittsburgh, Department of Chemistry and
Center for Molecular and Materials Simulations, Chevron Science Center, 219 Parkman Ave.,
Pittsburgh, Pennsylvania 15260

Received January 7, 2006; E-mail: jordan@pitt.edu

Abstract: It has been established that the excess electrons in small (i.e., $n \leq 7$) $(\text{H}_2\text{O})_n^-$ clusters are bound in the dipole field of the neutral cluster and, thus, exist as surface states. However, the motifs for the binding of an excess electron to larger water clusters remain the subject of considerable debate. The prevailing view is that electrostatic interactions with the “free” OH bonds of the cluster dominate the binding of the excess electron in both small and large clusters. In the present study, a quantum Drude model is used to study selected $(\text{H}_2\text{O})_n^-$ clusters in the $n = 12$ –24 size range with the goal of elucidating different possible binding motifs. In addition to the known surface and cavity states, we identify a new binding motif, where the excess electron permeates the hydrogen-bonding network. It is found that electrostatic interactions dominate the binding of the excess electron only for isomers with large dipole moments, whereas in isomers without large dipole moments polarization and correlation effects dominate. Remarkably, for the network-permeating states, the excess electron binds even in the absence of electrostatic interactions.

Introduction

Ever since the detection of $(\text{H}_2\text{O})_n^-$ ions mass spectroscopically,¹ there has been considerable interest in the nature of the excess electron in these clusters.^{2–9} In particular, the question of whether the excess electron is on the surface or in the interior of the clusters has been the subject of much speculation.^{2–4,8} Recently, there has been a flurry of new experimental and theoretical studies of $(\text{H}_2\text{O})_n^-$ ions.^{10–18} Particularly intriguing are the photoelectron spectra for the $(\text{H}_2\text{O})_n^-$, $n = 11$ –150, clusters obtained by the Neumark group.¹⁵ These spectra show three distinct features the relative intensities of which depend

on the source conditions and on the cluster size n . On the basis of theoretical results of Barnett et al.,³ these features were interpreted as arising from three distinct isomer classes, where the feature with the largest electron binding energies (isomer I) was attributed to an isomer with the excess electron bound in the interior of the cluster and those with the smaller electron binding energies were attributed to isomers (isomers II and III in ref 15) with the excess electron in surface states.¹⁵ Yet, a recent theoretical study of $(\text{H}_2\text{O})_n^-$ clusters by Turi et al.¹⁶ found that at temperatures of 200 and 300 K only surface states were stable for the $n = 20$ –104 clusters, and that for $T = 100$ K only the $n \geq 45$ clusters had stable interior states. This led these authors to conclude that all isomers observed experimentally are surface states, a view that was immediately challenged by Bragg et al.¹⁸ Thus, despite the long standing interest in water cluster anions, the electron binding motifs of all but the smallest systems¹⁰ remain controversial.

The conventional wisdom is that the binding of excess electrons to water clusters, in water films, and in bulk water is dominated by electrostatic interactions between the excess electron and the charge distributions of the water monomers. As a result, it is expected that in the anionic clusters, the “free” OH groups (i.e., those not engaged in H-bonds) of the water molecules are geometrically arranged so as to generate a region on the surface or in the interior of the cluster with a net attractive electrostatic potential. Indeed, for the $(\text{H}_2\text{O})_n^-$, $n = 2$ –7, clusters, it has been established that the most abundant anions observed experimentally are dipole-bound species (for recent reviews of dipole-bound anions, see refs 19 and 20), with the excess electron localized on the surface of the cluster, in the

- (1) Haberland, H.; Ludewigt, C.; Schindler, H. G.; Worsnop, D. R. *J. Chem. Phys.* **1984**, *81*, 3724.
- (2) Coe, J. V.; Lee, G. H.; Eaton, J. G.; Arnold, S. T.; Sarkas, H. W.; Bowen, K. H.; Ludewigt, C.; Worsnop, D. R. *J. Chem. Phys.* **1990**, *92*, 3980.
- (3) Barnett, R. N.; Landman, U.; Scharf, D.; Jortner, J. *Acc. Chem. Res.* **1989**, *22*, 350.
- (4) Barnett, R. N.; Landman, U.; Nitzen, A. *J. Chem. Phys.* **1989**, *91*, 5567.
- (5) Kim, K. S.; Park, I.; Lee, S.; Cho, K.; Lee, J.; Joannopoulos, J. D. *Phys. Rev. Lett.* **1996**, *76*, 956.
- (6) Ayotte, P.; Weddle, G. W.; Bailey, C. G.; Johnson, M. A.; Vila, F.; Jordan, K. D. *J. Chem. Phys.* **1999**, *110*, 6268.
- (7) Kim, J.; Becker, I.; Cheshnovsky, O.; Johnson, M. A. *Chem. Phys. Lett.* **1998**, *297*, 90.
- (8) Coe, J. V. *Int. Rev. Phys. Chem.* **2001**, *20*, 33.
- (9) Jordan, K. D. *Science* **2004**, *306*, 618.
- (10) Hammer, N. I.; Shin, J. W.; Headrick, J. M.; Kiden, E. G.; Roscioli, J. R.; Weddle, G. H.; Johnson, M. A. *Science* **2004**, *306*, 675.
- (11) Hammer, N. H.; Roscioli, J. R.; Johnson, M. A. *J. Phys. Chem. A* **2005**, *109*, 7896.
- (12) Shen, J.-W.; Hammer, N. H.; Headrick, J. M.; Johnson, M. A. *Chem. Phys. Lett.* **2004**, *399*, 3419.
- (13) Paik, D. H.; Lee, I. R.; Yang, D. S.; Baskin, J. S.; Zewail, A. H. *Science* **2004**, *306*, 672.
- (14) Bragg, A. E.; Verlet, J. R. R.; Kammrath, A.; Cheshnovsky, O.; Neumark, D. M. *Science* **2004**, *306*, 669.
- (15) Verlet, J. R. R.; Bragg, A. E.; Kammrath, A.; Cheshnovsky, O.; Neumark, D. M. *Science* **2005**, *307*, 93.
- (16) Turi, L.; Sheu, W. S.; Rossky, P. J. *Science* **2005**, *309*, 914.
- (17) Blau, S. K. *Physics Today* **2005**, *58*, 21.
- (18) Bragg, A. E.; Verlet, J. R.; Kammrath, A.; Cheshnovsky, O.; Neumark, D. M. *J. Am. Chem. Soc.* **2005**, *127*, 15283.

- (19) Compton, R. N.; Hammer, N. I. *Advances in Gas-Phase Ion Chemistry*; JAI Press: Stamford, Connecticut, 2001; Vol. 4, p 257–305.
- (20) Jordan, K. D.; Wang, F. *Annu. Rev. Phys. Chem.* **2003**, *54*, 367.

vicinity of a water monomer with two free OH groups.^{10–12} At the other extreme, there is strong evidence that the hydrated electron (e_{aq}^-), an electron in bulk water, is bound inside a roughly spherical cavity with the water molecules in the first “solvation” shell having free OH groups oriented toward the center of the cavity.²¹

However, the above picture, which focuses on electrostatics, cannot be the whole story, as it is now well established that electron correlation plays an essential role in the binding of an excess electron to polar molecules and their clusters.^{20,22} For example, for typical $(\text{H}_2\text{O})_6^-$ isomers, about 50% of the binding energy of the excess electron is due to electron correlation.²³ For the $(\text{H}_2\text{O})_6^-$ anions the dominant correlation effects arise from dispersion interactions between the diffuse excess electron and the more localized electrons of the polar molecules.^{20,22} Nevertheless, with one exception discussed below, the theoretical approaches used to examine the issue of surface vs. interior states of an excess electron bound to large ($n \geq 20$ water clusters) have neglected dispersion interactions as they have been based on one-electron model potentials (although some influence of correlation may be included implicitly through the parametrization of the model). Given the importance of correlation contributions for the binding of the excess electron, it is possible that there are electron binding motifs that cannot be described by approaches that do not explicitly include correlation.

The only studies that have included electron correlation in ab initio calculations on negatively charged water clusters larger than $n \geq 20$ are those of Herbert and Head-Gordon,^{24,25} who examined, using second-order Møller–Plesset perturbation theory (MP2), selected isomers of $(\text{H}_2\text{O})_n^-$ clusters with n as large as 24. This work confirmed the importance of electron correlation for binding an excess electron in both surface and cavity states. However, ab initio MP2 calculations on clusters of this size are very computationally demanding, and such calculations cannot be used to exhaustively explore the potential energy surface or to include the effects of temperature (through Monte Carlo or molecular dynamics simulations). Moreover, ab initio electronic structure methods do not permit zeroing out the electrostatic interactions in order to explore whether correlation effects alone can bind an excess electron.

In the present work, we use a quantum Drude oscillator model developed in our group^{23,26,27} to examine the role of electron correlation for different binding motifs of an excess electron to water clusters in the $n = 12–24$ size range. We investigate clusters with surface-bound and interior-bound excess electron states, and show that the relative contributions of electrostatic and correlation contributions to the electron binding energies are very different for these two classes of anions, implying that inclusion of correlation effects is essential for establishing the relative stability of surface vs. interior states. Moreover, we report a new binding motif, where the excess electron does not occupy a void or cavity, but rather permeates the H-bonding network. In these “network permeating states”, the binding of the excess electron derives almost entirely from

electron correlation as is demonstrated through the results obtained by switching off the electrostatic interactions in the model potential.

Methodology

In the Drude model for excess electrons bound to water clusters, the polarizable charge density of each water monomer is modeled by a quantum Drude oscillator, which consists of two point particles with opposite charges $+q_D$ and $-q_D$ that interact with each other through a harmonic potential with force constant k_D . By treating the electron–Drude oscillator interactions quantum mechanically, both electron–water polarization and electron–water dispersion interactions are explicitly included. This can be viewed as a coarse graining approach in which the 10 electrons of each water monomer are modeled by a three-dimensional Drude oscillator.

The implementation of the Drude model used in this work employs the Dang–Chang water model²⁸ to describe the water–water interactions and the electron–water electrostatics. The Dang–Chang water model employs on each monomer three point charges (0.519 on each H atom and -1.180 on the so-called M site, located on the rotational axis and displaced 0.215 \AA from the O atom toward the H atoms), and a single isotropic polarizable center also located at the M site. It also includes Lennard–Jones interactions between the O atoms of different water monomers. In the Drude model, the polarizable site on each monomer is replaced by a Drude oscillator, the polarizability of which, $\alpha_D = q_D^2/k_D$, is chosen to be equal to the experimental polarizability of the water monomer (9.745 au).²⁹ The Hamiltonian for the excess electron allows for interactions with the point charges and with the intermolecular induced dipoles, as well as for coupling with the Drude oscillators. It also includes terms to account for the short-range repulsion between the excess electron and the monomers. More details regarding the quantum Drude model and the numerical aspects of the calculations can be found in refs 23, 26, 27, and 30. Extensive tests on water clusters containing up to seven water monomers have shown that the Drude model gives electron binding energies very close to those of high-level coupled cluster electronic structure calculations with flexible basis sets.^{23,31}

Results

In this section, we report electron binding energies and the distributions of the excess electron for a set of prototypical water clusters. The electron binding energies have been computed at three levels of theory which we refer to as follows: (1) electrostatic (ES), which includes interactions of the excess electron with the permanent charges and intermolecular induced dipole moments on the water monomers, as well as with the short-range repulsive potentials but does not include polarization of the water molecules by the excess electron or correlation between the excess electron and the Drude oscillators, (2) second-order perturbation theory (PT2) which includes, in addition to the interactions in the ES treatment, polarization and dispersion interactions between the excess electron and the Drude oscillators, and (3) configuration interaction (CI) which includes all the interactions present in the PT2 approximation as well as higher-order correlation effects between the excess electron and the Drude oscillators.

It should be noted that the PT2 calculations carried out using the Drude model do not directly correspond to ab initio MP2 calculations, since the zeroth-order wave functions differ in the

(21) Tauber, M. J.; Mathies, R. A. *J. Am. Chem. Soc.* **2003**, *125*, 1394.

(22) Gutowski, M.; Skurski, P.; I., B. A.; Simons, J.; Jordan, K. D. *Phys. Rev. A* **1996**, *54*, 1906.

(23) Wang, F.; Jordan, K. D. *J. Chem. Phys.* **2003**, *119*, 11645.

(24) Herbert, J. M.; Head-Gordon, M. *J. Phys. Chem.* **2005**, *109*, 5217.

(25) Herbert, J. M.; Head-Gordon, M. *Phys. Chem. Chem. Phys.* **2006**, *8*, 68.

(26) Wang, F.; Jordan, K. D. *J. Chem. Phys.* **2001**, *114*, 10717.

(27) Wang, F.; Jordan, K. D. *J. Chem. Phys.* **2002**, *116*, 6973.

(28) Dang, L. X.; Chang, T. M. *J. Chem. Phys.* **1996**, *106*, 8149.

(29) Stillinger, F. H. *The Liquid State of Matter; Fluids, Simple and Complex*; North-Holland: Amsterdam, 1992.

(30) Sommerfeld, T.; Jordan, K. D. *J. Phys. Chem.* **2005**, *109*, 11531.

(31) Diri, K.; Jordan, K. D. unpublished work.

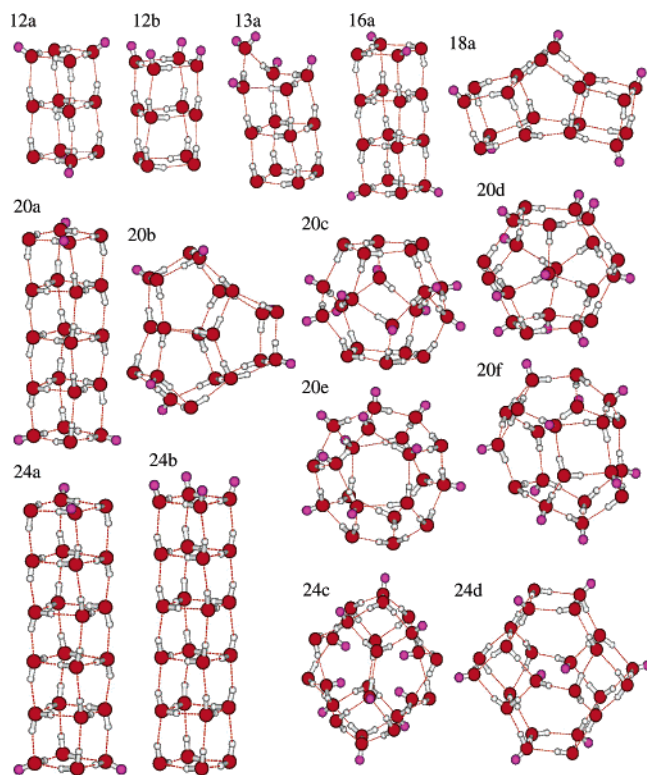


Figure 1. Structures of 15 selected water cluster anions examined in this study. The H atoms of free OH groups are colored purple.

two approaches. First, the ab initio Hartree–Fock wave function overestimates the dipole moment of the water monomer by about 0.2 D, whereas the Drude model, by design, employs charges that reproduce the experimental value of the dipole moment of the neutral monomer. Second, the Hartree–Fock reference function used in ab initio MP2 calculations already includes polarization of the water molecules by the excess electron, whereas these appear as a second-order correction in the present implementation of the Drude model.

The clusters considered are depicted in Figure 1 and include the $n = 12, 16, 20,$ and 24 fused-cubic isomers (12a, 12b, 16a, 20a, 24a, and 24b), a pentagonal prism isomer of $(\text{H}_2\text{O})_{20}^-$ (20b), and a $(\text{H}_2\text{O})_{18}^-$ isomer consisting of a prism fused to two cubes (18a). Apart from 12b and 24b, these structures correspond to low-energy isomers of the neutral clusters. Isomers 12a, 16a, 18a, and 20b, in fact, have structures that correspond to those of the global minima of the respective neutral clusters^{26,32,33} (other than the small relaxation brought about by the attached electron). In addition, we include a structure with a double-acceptor monomer (13a), three dodecahedral isomers (20c–e) and a $(4^5 4^6 2)$ isomer (20f) of $(\text{H}_2\text{O})_{20}^-$, as well as two $(\text{H}_2\text{O})_{24}^-$ isomers with either four (24c) or two (24d) OH groups pointing toward the center of the cluster and which thus can support cavity states. Structures 20e, 20f, 24c, and 24d have been considered previously by Khan³⁴ and by Herbert and Head-Gordon.^{24,25} Apart from 20c, all geometries were optimized for the cluster anions using the Drude model and the CI method. 20c is included as an example of a cluster where the electron binds to the surface even though the net dipole moment is zero.

Table 1. Total Energies, Dipole Moments, Electron Binding Energies, and Reduced Electron Densities of Selected Water Cluster Anions^a

cluster	E_{tot} [meV]	μ (D ^b)	electron binding ^c energy (meV)			I_p ^d [%]
			ES	PT2	CI	
12a	−4730	0	−5	−4	47.5	1
12b	−5029	19.6	640	1029	1212	68
13a	−5419	23.0	812	1236	1374	71
16a	−6651	0	−5	−4	138	14
18a	−7636	3.3	−1	5.2	242	30
20a	−8611	0	−5	−4	248	27
20b	−8540	0.4	−5	−4	138	11
20c	−7258	0	−4	0.1	182	0
20d	−7869	4	0	7.9	170	20
20e	−7957	25.6	687	1070	1252	66
20f	−8019	6.3	20.4	68	251	36
24a	−10530	0.2	−5	−4	289	31
24b	−10890	44.8	1175	1702	1908	71
24c	−9875	0	−5	−4	867	75
24d	−10147	0	−5	−3	725	68

^a All results from calculations using the Drude model. ^b The dipole moments are for the associated neutral clusters. ^c Bound anions are indicated by positive binding energies. Physical significance should not be attributed to the negative binding energies. ^d I_p is the percentage of the charge distribution of the excess electron as described by the CI calculations contained within the 2×10^{-4} Bohr^{−3} isosurface.

Optimization of the geometry of the anion of 20c results in a rearrangement to a structure for which the associated neutral cluster has a sizable dipole moment.

Table 1 summarizes the total binding energies [relative to n water monomers and a free 0 eV electron] and electron binding energies of the anions as well as the dipole moments of the neutral frameworks for the clusters depicted in Figure 1. Table 1 also reports the percentage of charge distribution (I_p) of the excess electron contained within the 2×10^{-4} Bohr^{−3} isosurface calculated at the CI level. The distributions of the excess electron obtained at the CI level are shown in Figure 2, where, with the exception of 12a and 20c, the isosurfaces correspond to an electron density of 2×10^{-4} Bohr^{−3}. Isomers 12a and 20c have very diffuse electron densities, and for these two systems the iso-surfaces are drawn at 1×10^{-4} Bohr^{−3} which encloses 12 and 20% of the density, respectively.

It is clear from the results summarized in Table 1 and from the charge distributions depicted in Figure 2 that 12b, 13a, 20e, 20f, and 24b are dipole-bound states, with the excess electron localized at the surface of the cluster and that 24c and 24d are cavity bound as over two-thirds of the charge density associated with the excess electron is localized in the interior of the cluster. However, there are also clusters (12a, 16a, 20a, 20b, and 24a) for which the maximum of the charge distribution occurs in the interior of the cluster, but for which most of the density of the excess electron is located outside the cluster. We refer to these as network permeating states. Moreover, some clusters (20c and 20d) form surface states despite the small or vanishing dipole, and there are clusters (e.g., 18a) for which the electron binding motif is intermediate between the latter two scenarios.

Structures with substantial (i.e., $\mu > 5$ D) dipole moments bind an excess electron even when only electrostatic interactions are considered, whereas those structures with small or vanishing net dipole moments (12a, 16a, 20a, 20c, 24a, 24c, and 24d) do not. It should be noted that in the Born–Oppenheimer approximation all clusters with dipole moments greater than 1.625 D should have an infinity of bound states, albeit with very small

(32) Wales, D. J.; Hodges, M. P. *Chem. Phys. Lett.* **1998**, 286.

(33) Hartke, B. *Phys. Chem. Chem. Phys.* **2003**, 5, 275.

(34) Khan, A. J. *Chem. Phys.* **2003**, 118, 1684.

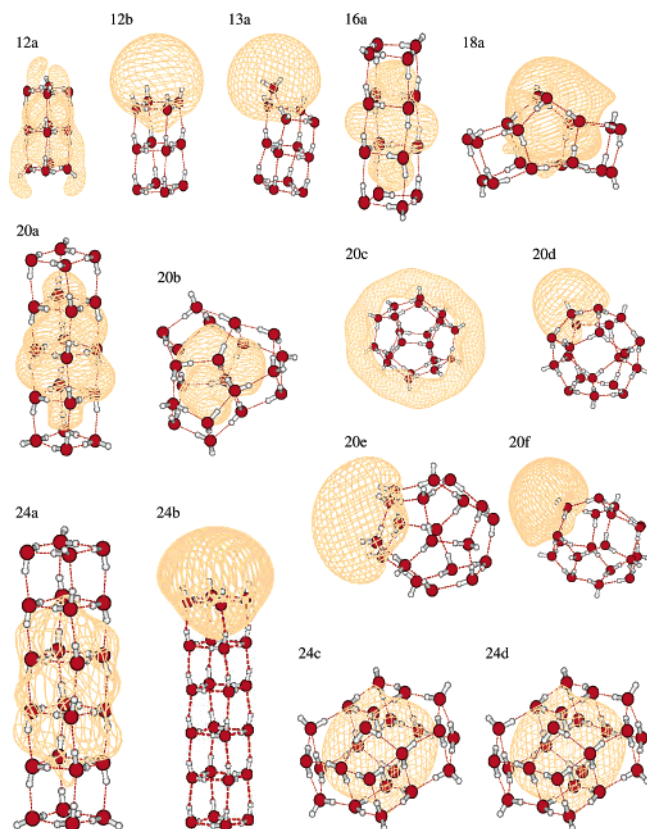


Figure 2. Distribution of the excess electron for the various water cluster anions. Shown are iso-surfaces of the reduced electron density from the CI wave function. For 12a and 20c, the iso-surface are drawn at a density of $1 \times 10^{-4} \text{ Bohr}^{-3}$, for all other clusters the iso-surface is at $2 \times 10^{-4} \text{ Bohr}^{-3}$.

electron binding energies when μ is in the 1.625 D – 5 D range.²⁰ The Gaussian basis sets used in this study are inadequate for describing these weakly bound states. However, this is not a problem as appreciable electron binding (i.e., greater than 47 meV) is found for all clusters considered when high-order correlation effects are included.

Inclusion of correlation at the PT2 level yields substantially increased electron binding energies for the large-dipole species, while most of the small (or zero)-dipole species do not bind the excess electron even at the PT2 level. The 18a ($\mu = 3.3$ D) and 20d ($\mu = 4$ D) clusters are intermediate in nature, and the PT2 method gives for these clusters very small electron binding energies of 5 and 8 meV, respectively. However, inclusion of higher-order electron correlation effects leads to appreciable (148–237 meV) enhancements of the electron binding energies of clusters with small (i.e., < 5 D) and large (> 5 D) dipole moments (Table 1).

The behavior described for the water clusters with large dipole moments is typical for dipole-bound states in general.²² Going from the ES treatment to the CI level of theory, the electron binding energies increase significantly (with the increase ranging from 70% for 13a up to a factor of about twelve for 20f). In general, the relative importance of high-order correlation effects grows with decreasing dipole moment. Analysis of the CI wave functions reveals that the enhanced binding is a consequence of configurations with the excess electron excited but with all Drude oscillators in their ground states. These configurations cause a large contraction of the charge distribution,^{27,30} but since they mix only indirectly into the zeroth-order wave function

through coupling with double excitations, this effect is not recovered in the PT2 treatment. For all dipole-bound species, the excess electron is localized at the surface of the cluster, in the vicinity of two or more free OH groups of surface monomers pointed toward the excess electron. Structural arrangements that lead to particularly strong binding are those with double-acceptor monomers (13a) or with multiple proximal double-acceptor single-donor water molecules orienting their free OH groups in roughly the same direction (12b and 24b).

The clusters with zero or near zero dipole moments behave quite differently. For none of these clusters is the electrostatic potential strong enough to bind an excess electron. Inclusion of the second-order dispersion interactions also does not lead to binding, with the exception of 20c, for which the excess electron is predicted to be bound in a surface state with 0.09 meV electron binding energy (EBE) at the PT2 level of theory. Only at the CI level, where higher-order correlation corrections cause contraction of the electron density, do we find appreciable electron binding energies for the clusters with zero or small dipole moments. This group of clusters includes the surface bound state of 20c (EBE = 182 meV), the cavity-bound anions 24c and 24d (EBE = 725 and 862 meV, respectively), and the network permeating species (12a, 16a, 18a, 20a, 20b, and 24a) with electron binding energies ranging from 47 to 289 meV. The latter clusters do not have any region on their surface or in their interior where free OH groups create an appreciably attractive electrostatic potential well for an excess electron. For these clusters, most of the density of the excess electron resides outside the cluster (see, Table 1), although the maxima of the electron densities are localized inside the hydrogen bonded network. We discuss below the factors responsible for the shape of these charge distributions. Note that the absolute contribution of electron correlation to the electron binding energies is greater for the cavity states than for the surface or network permeating states.

To further explore the interplay of correlation and electrostatics, we have carried out a series of calculations in which the electrostatic interactions between the excess electron and the cluster are gradually switched off, keeping the geometries fixed. This is accomplished by introducing a scaling factor, α , for the point charges in the Dang–Chang water model. For $\alpha = 0$, the electronic Hamiltonian includes only the short-range repulsive potential associated with the excluded volume of each water monomer and the interactions of the excess electron with the Drude oscillators, whereas for $\alpha = 1$, the electronic Hamiltonian includes as well the “full” charges and induced dipoles.

Figure 3 reports the variation of the electron binding energies as a function of α for a chain isomer of $(\text{H}_2\text{O})_6^-$, which is a prototypical dipole-bound species, the network permeating isomer 16a, a cavity state 24c, and 20d for which the orbital of the excess electron changes from surface to network permeating character as α is decreased. The chain isomer of $(\text{H}_2\text{O})_6^-$ is employed for this purpose, since it represents a “pure” dipole-bound state that cannot change into network permeating for small α . As expected, electrostatic interactions are crucial for the dipole-bound species. As the strength of the electrostatic potential is reduced, the electron binding energy rapidly decreases to zero. In contrast, the electron binding energy of the network permeating state of 16a is essentially independent of the strength of the electrostatic interactions, underscoring that

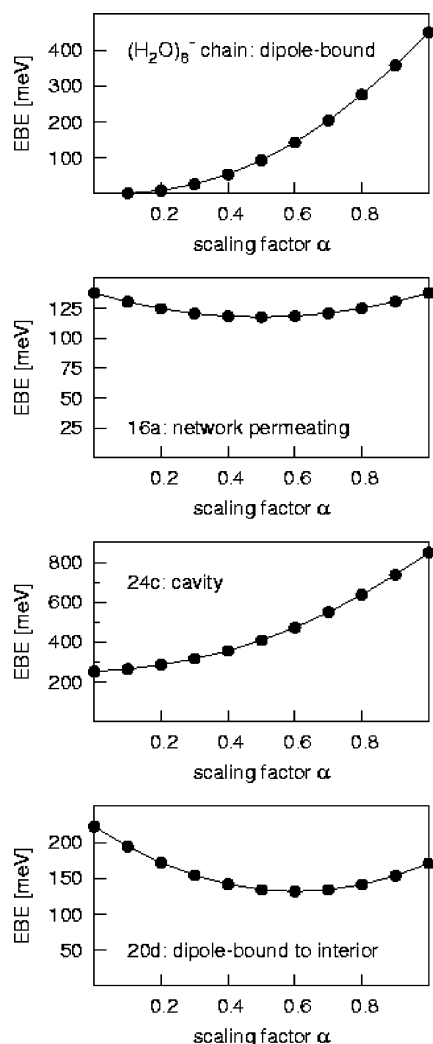


Figure 3. Electron binding energy (EBE) of the chain isomer of $(\text{H}_2\text{O})_6^-$, and of 16a, 20d, and 24c as a function of the strength of the electrostatic interaction between the water monomers and the excess electron.

the binding of the excess electron to this cluster is almost entirely due to correlation effects. For other correlation-bound excess electron species, see refs 35 and 36. The cavity state of 24c displays intermediate behavior in that its binding energy decreases as the electrostatic interactions are decreased; however, it does not drop to zero, but rather, remains at about 30% of its original value as $\alpha \rightarrow 0$. This shows that the attractive electrostatic well in the interior of the cluster contributes substantially to the electron binding.

The interplay between the different binding motifs is illustrated by the dodecahedral isomer 20d. With $\alpha = 1$, this cluster has a dipole moment of 4 D, and the excess electron binds as a dipole-bound surface state. When the electrostatic interactions are turned off, the excess electron state is converted to a network permeating state with a larger electron binding energy than the original dipole-bound state. (See Figure 4.) This network permeating state is not found when the electrostatic interactions are present because the dipole moments of the monomers are aligned so as to destabilize an electron with appreciable weight in the cavity. An analogous situation is found for 20c for which the surface bound state converts to a network permeating state when the electrostatic interactions are turned off.

The above analysis provides a physical picture of the origin

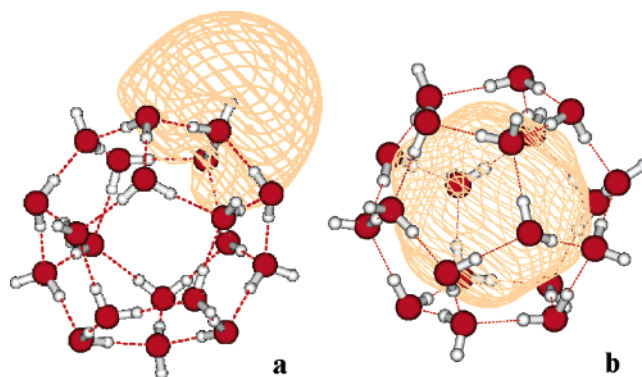


Figure 4. Change in the nature of the electron binding of 20d when electrostatics are turned off. (a) full electrostatics, and (b) electrostatic interactions between the excess electron and the water molecules are turned off.

of the unique charge distributions of the network permeating states. Namely, since electrostatics play a negligible role for these species, the binding of the excess electron arises almost entirely from correlation effects. Dispersion and higher-order correlation effects are attractive both in the interior and on the exterior of the cluster. It is essentially the free space available inside the H-bonding network that determines the portion of the charge density found in the interior of the cluster. This portion grows with increasing cluster size as seen from the results summarized in Table 1 and in Figure 2.

Conclusions

We have studied the binding of an excess electron to selected water clusters with 12 to 24 monomers. Three major binding motifs can be distinguished: (1) surface states, (2) cavity states, and (3) network permeating states. In the surface states the excess electron localizes in the vicinity of OH groups protruding from the neutral cluster, and the excess electron is bound even in the absence of polarization and correlation interactions unless the dipole-moment is small (see, for example, 20c). However, correlation contributions significantly enhance the electron binding energies. Examples for structures that lead to strongly bound surface states include double-acceptor waters (e.g., 13a) and species with several nearby water molecules with free OH groups pointed away from the surface in roughly the same direction.

Cavity states can result when several water molecules point free OH groups toward the center of a cavity in the H-bonded network. Despite this favorable electrostatic situation, for such clusters considered here, the electrostatic (plus repulsive) potential does not bind an excess electron. Even with inclusion of second-order dispersion interactions, the excess electron remains unbound. Only when higher-order electron correlation effects are included are sizable electron binding energies calculated. Nevertheless, electrostatic interactions do make a significant contribution to the electron binding energies of the cavity states, as is demonstrated by the smaller electron binding energies found when electrostatic interactions are turned off.

In the network permeating states, the excess electron is not associated with free OH groups, but rather is delocalized over the cluster, with the maxima of the electron density occurring within the three-dimensional hydrogen bonding network, but

(35) Skurski, P.; Rak, J.; Simons, J. *J. Chem. Phys.* **2001**, *115*, 11193.

(36) Sommerfeld, T. *J. Chem. Phys.* **2004**, *121*, 4097.

with most of the electron density occurring outside the cluster. In these species, the electron binding is essentially independent of electrostatic interactions, i.e., it is dominated by correlation effects. Ab initio calculations will be a great challenge for these species as use of a large diffuse basis set and inclusion of high-order correlation effects are necessary for describing the electron binding. Moreover, ab initio MP2 calculations may not be viable, owing to the lack of a suitable Hartree–Fock reference wave function for the anion analogous to the succino-nitrile anion case.³⁶

The three electron binding motifs are not mutually exclusive. Indeed, we have found one example (18a) that is intermediate between surface-bound and network permeating. The binding energies of the network permeating states tend to be appreciably smaller than those of the dipole- or cavity-bound states, and the electron densities are accordingly more diffuse. Despite their relatively small electron binding energies, network permeating states may play an important role in the electron attachment to gas phase $(\text{H}_2\text{O})_n$ clusters, since the low-energy isomers of the neutral clusters lack cavities and possess small dipole moments.^{32,33} They may also play a role funneling excess electrons toward more tightly bound dipole-bound or cavity-bound excess electron states.

It is interesting to speculate on the fate of a water cluster following electron capture. Assuming that the starting neutral cluster has zero or a small dipole moment, the initially formed anion is expected to be in a weakly bound surface state or a network permeating state. The resulting anion can rearrange into structures with lower total energies and larger electron binding energies, for example, via donor–acceptor exchanges of adjacent water monomers.³⁷ For the cluster sizes considered here, the most stable structures are expected to have the excess electron in dipole-bound surface states, since the anions with the excess electron bound in the interior are energetically very unfavorable compared to the most stable neutral clusters. A schematic of a typical rearrangement pathway is shown in Figure 5. As one moves from left to right in the figure, one encounters neutral clusters with increasingly large dipole moments, and, thus, more strongly bound anions. For the formation of long-lived or stable anions, the early barriers will be decisive, since in this region of nuclear configuration space, the potential energy surfaces of the neutral and anionic clusters are close, and rearrangement into more strongly bound anions may be suppressed by electron autodetachment. This picture of the electron capture process suggests a straightforward explanation for the observed tem-

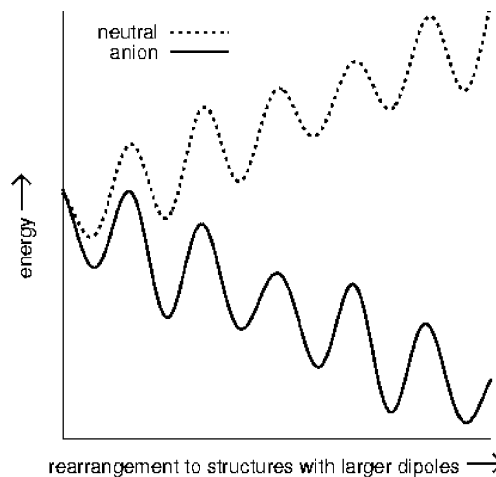


Figure 5. Schematic representation of the potential energy surface of a water cluster and its corresponding anion. Low-energy isomers of the neutral cluster tend to have small dipole moments, whereas the most stable forms of the anion tend to have large dipole moments (for the underlying neutral cluster).

perature dependence of the photoelectron spectra: namely, lower cluster temperatures lead to trapping in one of the early minima with small electron binding energies, along the reaction pathway.

The goal of the present study has been to characterize different motifs for the binding of an excess electron to water clusters rather than to identify the specific isomers observed in recent experiments.¹⁵ Nonetheless, it is relevant to note that for the cluster sizes considered in the present study, there are isomers with dipole-bound surface states that are much more stable and have much larger electron binding energies than the isomers with the excess electron bound in the interior of the cluster. This leads us to conclude that experimentally observed clusters with large electron binding energies are not necessarily due to cavity bound states as was noted also by Turi et al.¹⁶ We note also that there are several types of anions with VDEs ≤ 300 meV that are candidates for the experimentally observed isomer III.¹⁵ These include surface states of isomers with no or small dipole moments as well as network permeating states.

Acknowledgment. This research was carried out with the support of the National Science Foundation (CHE518253) and the Department of Energy (DE-FG02-00ER15066). We acknowledge valuable discussions with Drs. Johnson, Herbert, Head-Gordon, and Simons.

(37) Myshakin, E. M.; Diri, K.; Jordan, K. D. *J. Phys. Chem.* **2004**, *108*, 6758.